Evidence for transformation from #T_c to #I pinning in MgB_2 by graphene oxide doping with improved low and high field J_c and pinning potential

F. X. Xiang, X. L. Wang, X. Xun, K. S. B. De Silva, Y. X. Wang, and S. X. Dou

Citation: Appl. Phys. Lett. **102**, 152601 (2013); doi: 10.1063/1.4799360
View online: http://dx.doi.org/10.1063/1.4799360
View Table of Contents: http://aip.scitation.org/toc/apl/102/15
Published by the American Institute of Physics

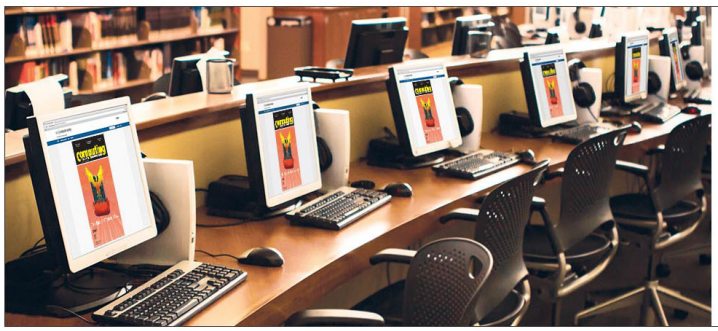

Evidence for transformation from δT_c to δl pinning in MgB_2 by graphene oxide doping with improved low and high field J_c and pinning potential

F. X. Xiang, X. L. Wang,[a] X. Xun, K. S. B. De Silva, Y. X. Wang, and S. X. Dou[a]
Institute for Superconducting and Electronic Materials, Australian Institute for Innovative Materials, Faculty of Engineering, University of Wollongong, Squires Way, North Wollongong, NSW 2500, Australia

(Received 3 December 2012; accepted 19 March 2013; published online 17 April 2013)

Flux pinning mechanism of graphene oxide (GO) doped MgB_2 has been systematically studied. In the framework of the collective pinning theory, a B-T phase diagram has been constructed. By adjusting the GO doping level, the pinning mechanism in MgB_2 transformed from transition temperature fluctuation induced pinning, δT_c pinning, to mean free path fluctuation induced pinning, δl pinning, is observed. Furthermore, in terms of the thermally activated flux flow model, the pinning potential in high field ($B > 5$ T) is enhanced by GO doping. The unique feature of GO is the significant improvement of both low field J_c and high field J_c. © *2013 American Institute of Physics*. [http://dx.doi.org/10.1063/1.4799360]

In type-II superconductors, due to its short coherence length, the most effective elementary interaction between vortex and pinning center is core interaction, which originates from the coupling of locally distorted superconducting properties with the periodic variation of the superconducting order parameter. Inhomogeneities in different parameters cause different "elementary pinning mechanisms." There exists two predominant mechanisms of core pinning, i.e., δT_c pinning and δl pinning. Whereas δT_c pinning is caused by the spatial variation of the Ginzburg-Landau coefficient α associated with disorder in the transition temperature T_c, variations in the charge-carrier mean free path l near lattice defects are the main cause of δl pinning.[1,2] For MgB_2 superconductor, it has been shown that δT_c pinning is dominant in un-doped MgB_2 samples, and δl pinning is dominant in carbon doped MgB_2 bulks, while δT_c and δl pinning coexist in silicone oil doped bulk samples.[3–5] But the systematical transformation from δT_c to δl pinning has not been observed.

Thermal energy may allow flux lines jump from one pinning site to another, which causes the finite resistivity below the transition temperature. It manifests a field-dependent broadening of the resistive transition. This phenomenon is very prominent in high temperature superconductors (HTSs) because of their large anisotropy induced by the two-dimensional (2D) structure and high transition temperatures. With a layer structure and relatively high T_c, thermally activated flux flow (TAFF) also results in the field-dependent broadening of the resistive transition in MgB_2. But it exhibits different behaviour compared to the high temperature superconductors.[6–9] First, the pinning potential, U_0, is very large in low field, on the order of 10^4 K; second, it exhibits very strong field dependence in high field.[10] So far, research on MgB_2 has been focused on pristine samples, however, with only limited studies reported on doping effects on U_0.[11,12]

Due to lack of intrinsic pinning, the J_c value of pristine MgB_2 drops very fast in field.[13] Chemical doping by nano-SiC, Si, C, and other carbon or silicon containing dopants has shown positive effects on high field J_c enhancement; however, the self field and low field J_c, as well as T_c, deteriorate.[11,14–18] Recently, our team has found that graphene can improve J_c at self field and low field with very little reduction in T_c,[12,19,20] but its high field J_c is not competitive with that of nano-SiC doped one. Also, we very recently found the graphene oxide (GO) doping can improve both the low and the high field J_c, which is different from the above dopants.[21]

In this work, we represent systematical study on the flux pinning mechanism of GO doped MgB_2 with much improved low field and high field J_c. By analysis of the flux pinning mechanism, the vortex pinning diagram is derived. According to the collective pinning theory, by adjusting the doping level, the transformation from transition temperature fluctuation induced pinning, δT_c pinning, to mean free path fluctuation induced pinning, δl pinning, was observed. In addition, the pinning potential is enhanced in high field ($B > 5$ T) by GO doping.

Figures 1(a) and 1(b) show the magnetic field dependence of the critical current density J_c for the un-doped and 1 wt. % GO doped MgB_2 at various temperatures. Fig. 1(a) shows the high field J_c of the 1 wt. % GO doped sample is enhanced compared with the un-doped sample from 5 K up to 25 K. For example, at 5 K and 10 T, the J_c for the un-doped sample is about 100 A · cm^{-2}, approaching the irreversibility field, but with 1 wt. % GO doping, the J_c is as high as 5200 A · cm^{-2}, about 52 times greater. As shown in Fig. S1(b) of the supplemental material,[22] GO doping increases the impurity scattering, which can cause an increase in the upper critical field (H_{c2}) and higher irreversibility field (H_{irr}). In addition, the defects, smaller grain size, and/or strain caused by doping could also improve the J_c in field. The enhanced H_{irr} and H_{c2} are shown in the inset of Fig. 1(a). Fig. 1(b) presents the low field J_c for the un-doped and 1 wt. % GO doped samples. It can be seen that the low field J_c for 1 wt. % GO addition is also improved compared with the un-doped sample. It is believed that the enhancement of J_c at low field is due to the improvement in the grain connectivity,[23] and we used Rowell's model to calculate the effective conducting area or active fraction (A_F).[24] Normally using the methodology of Rowell to estimate connectivity

[a]Authors to whom correspondence should be addressed. Electronic addresses: xiaolin@uow.edu.au and shi@uow.edu.au

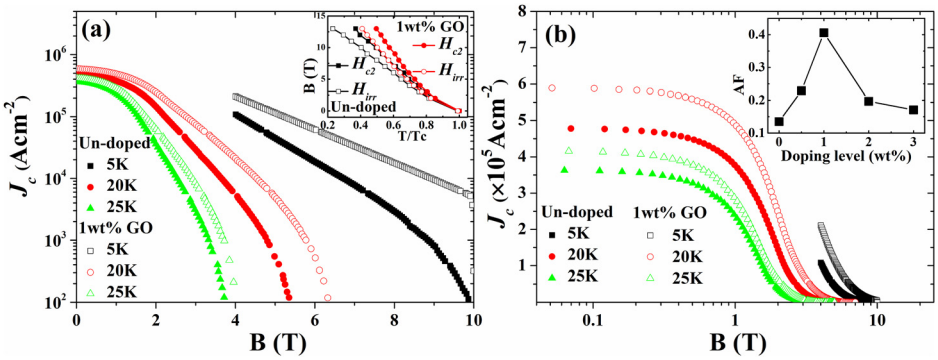

FIG. 1. (a) Log J_c vs. B for un-doped and 1 wt. % GO doped samples at various temperatures. The inset shows H_{c2} and H_{irr}, which were deduced 0.9 and 0.1 of $\rho(H,T)$. (b) J_c vs. log B for the un-doped and 1 wt. % GO doped samples at various temperatures. The top inset shows the J_c at 0.05 T for the un-doped and 1 wt. % GO doped samples, and the bottom inset shows that A_F varies with different doping levels.

suggests that few alloyed samples of MgB_2 have connectivity fractions that exceed 0.1.[25] In the inset in Fig. 1(b), it can be seen that the effective conducting area is improved by doping with GO, the 1 wt. % GO doped sample shows the best grain connectivity with A_F value of 0.4 comparing with 0.135 of un-doped sample. But after that the effective conducting area shows a decrease, which could be because a high concentration of GO decreases the volume of the superconducting phase.

When the pinning is induced by uncorrelated disorder, the collective pinning theory has been proven very successful in describing the vortex behavior and analyzing the corresponding vortex pinning mechanisms in high temperature superconductors and MgB_2.[1–3] According to this theory, the magnetic field dependence of J_c obeys different laws in different magnetic fields. First, when the magnetic field is smaller than B_{sb} (the crossover field from the single vortex to the small vortex bundle pinning regime), the J_c is field independent, exhibiting a plateau in the J_c–B diagram. Then, when $B > B_{sb}$ (in the small bundle pinning regime), $J_c(B)$ obeys an exponential law as

$$J_c(B) = J_c(0)\exp[-(B/B_0)^{3/2}], \quad (1)$$

where B_0 is a constant. In Fig. 2(a), we can observe the J_c plateau in the GO doped MgB_2 sample, which corresponds to the single vortex pinning regime. Using Eq. (1) for the small bundle pinning to fit the J_c curves, it can be seen that at intermediate field, the solid fitting lines fit the experimental data very well, while a deviation between the fitting line and the experimental data exists at low and high fields. In order to clearly determine the crossover field B_{sb} from the single vortex pinning regime to the small bundle pinning regime, the data were replotted on a double logarithmic plot as $-\ln(J_c(B)/J_c(0))$ vs. field, as shown in Fig. 2(b). At intermediate field, a straight line was clearly observed, corresponding to the small bundle pinning regime. The deviation at low field of the fitting line from the experimental data is B_{sb}. Meanwhile, the deviation at high field first is considered as the transition from the small bundle pinning to the large bundle pinning regime, although the high-field experimental data cannot be fitted by the power law of $J_c(B)$.

From Fig. 2(a), the irreversibility field, H_{irr}, can also be determined by the criterion $J_c = 100$ A cm^{-2}, which is shown in Fig. 2(c). These data can be fitted by the following equation:

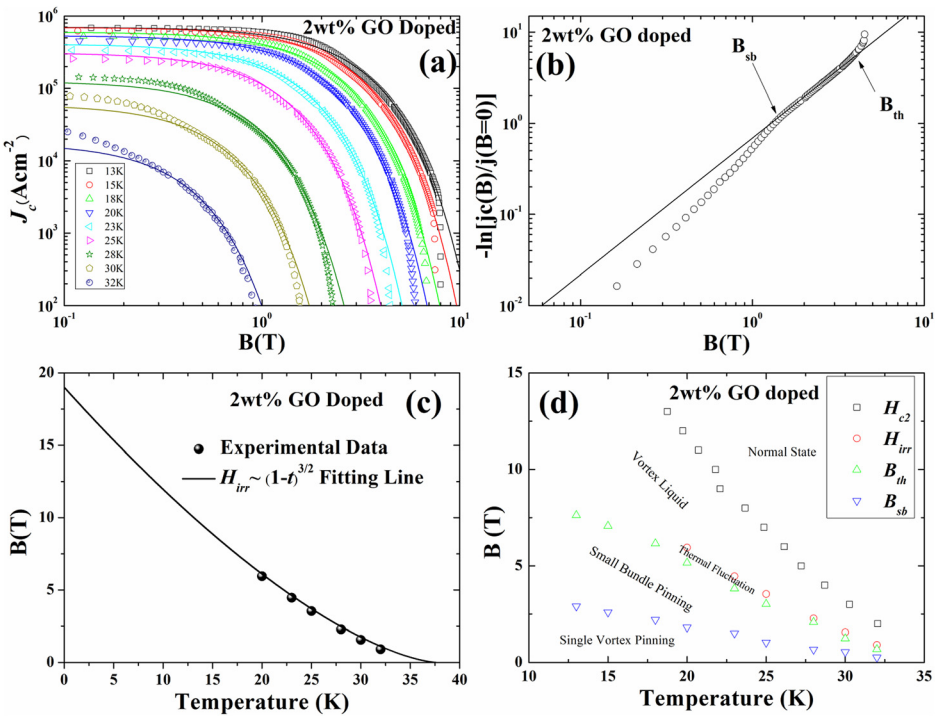

FIG. 2. (a) J_c at various temperatures for the 2 wt. % GO doped sample in a double logarithmic plot as log J_c vs. log B. The solid lines are fits based on Eq. (1). (b) J_c at 23 K for 2 wt. % GO doped sample in double logarithmic plot of $\ln[J_c(B)/J_c(0)]$ vs. log B. The solid line is the fitting line according to Eq. (1). (c) The irreversibility field obtained from the magnetic J_c curve by the criterion of 100 A · cm^{-2}. The solid line is a fit in terms of the giant creep model. (d) B-T phase diagram of 2 wt. % GO doped sample.

$$H_{irr}(t) = H_{irr}(0)(1-t)^{3/2}, \quad (2)$$

where $t = T/T_c$. The data indicate that giant flux creep also plays an important role in the 2 wt. % GO doped MgB_2 sample.[26]

After deriving the B_{sb}, the crossover field to the thermal fluctuation regime (B_{th}), H_{irr}, and H_{c2}, we can then try to construct the vortex phase diagram, as shown in Fig. 2(d), where H_{c2} is deduced using the criteria of 0.9 of $\rho(H,T)$ at the transition to superconductivity by measuring the resistivity at varying temperatures and fields. Below B_{sb}, there is a single vortex pinning regime, while the small bundle pinning regime is in between the B_{sb} and B_{th}. There exists a small regime between B_{th} and H_{irr} governed by the thermal fluctuation effect. Above the H_{irr} and below the H_{c2} is the vortex liquid pinning regime, and above the H_{c2}, there is the normal state regime. Compared with the un-doped sample, the GO doped sample shows a wider vortex phase region due to the enhanced flux pinning and H_{c2}, which also can be seen in silicone-oil-doped samples.[5]

Griessen *et al.*[27] derived that in the single vortex regime of a system with randomly distributed weak pinning centers, for δl pinning and δT_c pinning, the J_c obeys the following laws, respectively:

$$J_c(t)/J_c(0) = (1-t^2)^{5/2}(1+t^2)^{-1/2} \quad (3)$$

and

$$J_c(t)/J_c(0) = (1-t^{2)7/6}(1+t^2)^{-5/6}, \quad (4)$$

where $t = T/T_c$.

With this model, the δl pinning was found to be the dominant pinning mechanism in $YBa_2Cu_3O_{7-x}$ (YBCO) films, and δT_c pinning dominates in single domain (Y, Pr)123.[27,28] For MgB_2, δT_c pinning and δl pinning are, respectively, found in un-doped and carbon doped samples, and δT_c and δl pinning coexist in silicone oil doped bulk samples.[3–5] So far, however, there has been no report on systematical transformation of the pinning mechanism by using one dopant. Here, we observed that depending on the doping level of GO, the pinning mechanism is systematically transformed from δT_c to δl pinning. We used the two equations given above to fit the experimental data. Clearly, it can be seen that in Fig. 3(a), the data for the un-doped sample are well fitted by the δT_c pinning model, which is consistent with Ref. 3; in Fig. 3(b), the data for the 1 wt. % GO doped sample are in between the δT_c and δl fitting lines, which means that both δT_c and δl pinning play an important role; and Fig. 3(c) shows that the 2 wt. % GO doped sample is dominated by δl pinning. In Fig. 3(d), we use the normalized temperature dependence to give a clearer picture of the different temperature dependences of J_c for the un-doped, and the 1 wt. % and 2 wt. % GO doped samples. The transformation from the δT_c pinning to δl pinning is in a good agreement with the varying trend in the residual resistivity ratio (see Fig. S1(b) of the supplemental material).[22] That is, with increasing doping level, the RRR becomes smaller, and the electron scattering becomes stronger, therefore, decreasing the charge carrier mean free path and increasing the δl pinning. This result can be ascribed to the low dimensionality of GO, which carries both C and O into the MgB_2 formation process. The simultaneous formation of MgB_2 with C incorporation, in combination with the formation of highly dispersed MgO within the MgB_2 matrix, results in multiple types of pinning centers, which are GO doping level dependent. Therefore, through adjusting the doping level, the electron scattering intensity can be tuned effectively.

Now, let us discuss the GO doping effect on the pinning potential based on the TAFF model. The field-dependent broadening of the resistive transition for the layered superconductors is interpreted by the dissipation of energy caused

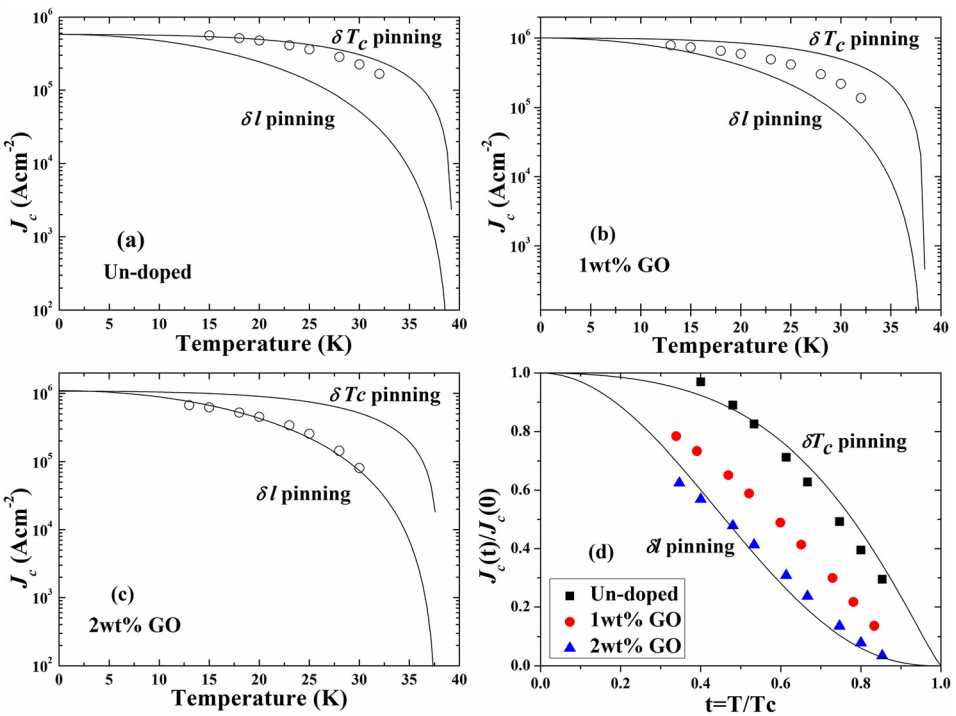

FIG. 3. Temperature dependence of J_c at 0.05 T for un-doped (a), 1 wt. % GO doped (b), and 2 wt. % GO doped (c) samples. The solid lines are the fits to the J_c curves in terms of the δl pinning and δT_c pinning mechanisms. (d) Normalized temperature dependence of J_c for un-doped, 1 wt. % GO doped, and 2 wt. % GO doped samples.

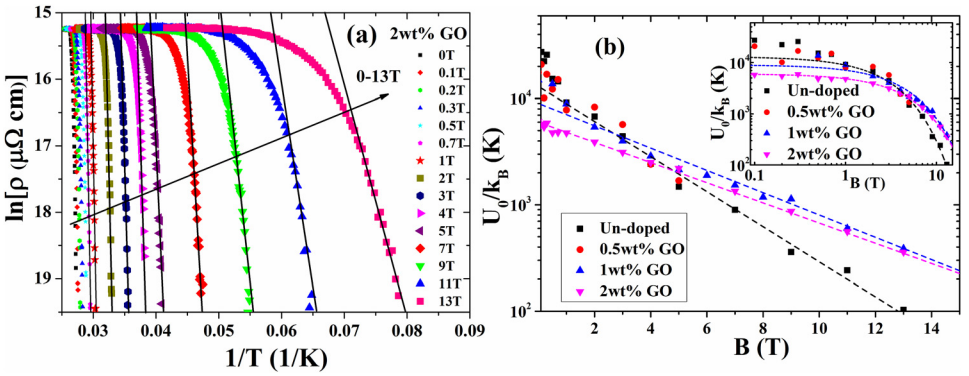

FIG. 4. (a) Arrhenius plot of the electrical resistivity of 2 wt. % GO doped MgB_2 at various fields up to 13 T. The solid lines are the fits of the linear part of the curves. (b) Field dependence of the pinning potential, U_0, for the un-doped, and the 0.5 wt. %, 1 wt. %, and 2 wt. % GO doped samples. The dashed lines are the fits corresponding to each sample. The inset shows a double logarithmic plot of U_0/k_B versus B.

by thermally activated flux flow, which can be described by the Arrhenius law, $\rho(T,B) = \rho_0 \exp[-U_0/k_B T]$, where U_0 is the flux-flow activation energy and deduced from the slope of the linear part of an Arrhenius plot, ρ_0 is a parameter, and k_B is Boltzmann's constant.[1,6] This phenomenon was previously observed in the layered cuprate superconductors, un-doped bulk and thin film MgB_2, and iron based superconductors,[6–10] but reports of doping effects on the pinning potential are very limited for MgB_2. Fig. S2 in the supplemental material shows that the T_c is broadened upon applying magnetic field.[22] The transition width, defined by 90% to 10% of the corresponding resistivity transition, is about 0.99 K at zero field, while it is 3.85 K in 13 T.[22] We replotted the data as lnρ vs. 1/T, as shown in Fig. 4(a). The linear part of the transition is clearly observed, corresponding to the thermally activated flux flow regime. The pinning potential U_0 is obtained by calculating the slope. The U_0 values of other samples are also obtained by the same method. In Fig. 4(b), our results show that the U_0 values of the un-doped and doped MgB_2 samples exhibit a plateau in low field (B < 1 T), but drop very fast in high field. In low fields, the pinning potential gradually decreases with increasing doping level. In high field, for the 0.5 wt. % GO doped sample, the field dependence of the pinning potential is similar to that of the un-doped sample; whereas for the 1 wt. % and 2 wt. % GO doping samples, the U_0 shows different field dependence and is much larger than for the un-doped sample in high field (B > 5 T). Compared with the power law field dependence of the activation energy, U_0 (B) $\propto B^{-n}$ with the exponent n < 1, which is usually observed for other layered systems, such as HTS and iron based superconductors,[6–9] MgB_2 shows similar behavior in low field, but in high field it exhibits a much stronger field dependence (B > 1 T), which is consistent with MgB_2 films. The strong field dependence in high field can be fitted by the exponential law: $U_0 \approx 10^{-kB}$, where k is the fitting parameter and B is the magnetic field. From the inset of Fig. 4(b), while there is deviation in low field between the fitting line and the experimental data for the un-doped, and the 0.5 wt. % and 1 wt. % GO doped samples, for the 2 wt. % sample, the fitting line is in good agreement with the experimental data both at low and at high fields.

In conclusion, we have systematically studied the flux pinning mechanism of GO doped MgB_2. By GO doping, J_c is enhanced significantly both at low and high fields, which is due to the improvements in grain connectivity, H_{irr}, and H_{c2}. In the framework of the collective pinning theory, a B-T phase diagram has been derived for GO doped MgB_2. By adjusting the GO level, the pinning mechanism transforms from δT_c to δl pinning. Furthermore, in terms of the TAFF model, the pinning potential in high field ($B > 5$ T) is enhanced by GO doping.

This work was supported by the Australian Research Council through Project Nos. DP0770205 and LP0989352. The authors thank Dr. G. Peleckis, Dr. W. X. Li, and Dr. T. Silver for assistance. This work was also supported by Hyper Tech Research, Inc., OH, USA.

[1]G. Blatter, M. V. Feigel'man, V. B. Geshkenbein, A. I. Larkin, and V. M. Vinokur, Rev. Mod. Phys. **66**, 1125 (1994).
[2]W. Roger, Rep. Prog. Phys. **62**, 187 (1999).
[3]M. J. Qin, X. L. Wang, H. K. Liu, and S. X. Dou, Phys. Rev. B **65**, 132508 (2002).
[4]J. L. Wang, R. Zeng, J. H. Kim, L. Lu, and S. X. Dou, Phys. Rev. B **77**, 174501 (2008).
[5]S. R. Ghorbani, X. L. Wang, S. X. Dou, S.-I. K. Lee, and M. S. A. Hossain, Phys. Rev. B **78**, 184502 (2008).
[6]T. T. M. Palstra, B. Batlogg, L. F. Schneemeyer, and J. V. Waszczak, Phys. Rev. Lett. **61**, 1662 (1988).
[7]T. T. M. Palstra, B. Batlogg, R. B. van Dover, L. F. Schneemeyer, and J. V. Waszczak, Phys. Rev. B **41**, 6621 (1990).
[8]X. L. Wang, A. H. Li, S. Yu, S. Ooi, K. Hirata, C. T. Lin, E. W. Collings, M. D. Sumption, M. Bhatia, S. Y. Ding, and S. X. Dou, J. Appl. Phys. **97**, 10B114 (2005).
[9]X.-L. Wang, S. R. Ghorbani, S.-I. Lee, S. X. Dou, C. T. Lin, T. H. Johansen, K. H. Müller, Z. X. Cheng, G. Peleckis, M. Shabazi, A. J. Qviller, V. V. Yurchenko, G. L. Sun, and D. L. Sun, Phys. Rev. B **82**, 024525 (2010).
[10]A. Sidorenko, V. Zdravkov, V. Ryazanov, S. Horn, S. Klimm, R. Tidecks, A. Wixforth, T. Koch, and T. Schimmel, Philos. Mag. **85**, 1783 (2005).
[11]J. Chen, V. Ferrando, P. Orgiani, A. V. Pogrebnyakov, R. H. T. Wilke, J. B. Betts, C. H. Mielke, J. M. Redwing, X. X. Xi, and Q. Li, Phys. Rev. B **74**, 174511 (2006).
[12]K. S. B. De Silva, X. Xu, S. Gambhir, X. L. Wang, W. X. Li, G. G. Wallace, and S. X. Dou, Scr. Mater. **65**, 634 (2011).
[13]Y. Bugoslavsky, G. K. Perkins, X. Qi, L. F. Cohen, and A. D. Caplin, Nature **410**, 563 (2001).
[14]S. X. Dou, S. Soltanian, J. Horvat, X. L. Wang, S. H. Zhou, M. Ionescu, H. K. Liu, P. Munroe, and M. Tomsic, Appl. Phys. Lett. **81**, 3419 (2002).
[15]X. L. Wang, S. H. Zhou, M. J. Qin, P. R. Munroe, S. Soltanian, H. K. Liu, and S. X. Dou, Physica C **385**, 461 (2003).
[16]J. H. Kim, S. Zhou, M. S. A. Hossain, A. V. Pan, and S. X. Dou, Appl. Phys. Lett. **89**, 142505 (2006).
[17]X. L. Wang, Z. X. Cheng, and S. X. Dou, Appl. Phys. Lett. **90**, 042501 (2007).
[18]X.-L. Wang, S. X. Dou, M. S. A. Hossain, Z. X. Cheng, X. Z. Liao, S. R. Ghorbani, Q. W. Yao, J. H. Kim, and T. Silver, Phys. Rev. B **81**, 224514 (2010).

[19]K. S. B. De Silva, S. Gambhir, X. L. Wang, X. Xu, W. X. Li, D. L. Officer, D. Wexler, G. G. Wallace, and S. X. Dou, J. Mater. Chem. **22**, 13941 (2012).
[20]K. S. B. De Silva, X. Xu, X. L. Wang, D. Wexler, D. Attard, F. Xiang, and S. X. Dou, Scr. Mater. **67**, 802 (2012).
[21]K. S. B. De Silva, S. H. Aboutalebi, X. Xu, X. L. Wang, W. X. Li, K. Konstantinov, and S. X. Dou, "Effects of graphene oxide doping on the superconducting properties of MgB_2" (unpublished).
[22]See supplementary material at http://dx.doi.org/10.1063/1.4799360 for experimental method, X-ray diffraction and resistivity results, and field-dependent broadening of transition temperature.
[23]M. Eisterer, Supercond. Sci. Technol. **20**, R47 (2007).
[24]M. R. John, Supercond. Sci. Technol. **16**, R17 (2003).
[25]Y. Iwasa, D. C. Larbalestier, M. Okada, R. Penco, M. D. Sumption, and X. X. Xi, IEEE Trans. Appl. Supercond. **16**, 1457 (2006).
[26]Y. Yeshurun and A. P. Malozemoff, Phys. Rev. Lett. **60**, 2202 (1988).
[27]R. Griessen, H.-h. Wen, A. J. J. van Dalen, B. Dam, J. Rector, H. G. Schnack, S. Libbrecht, E. Osquiguil, and Y. Bruynseraede, Phys. Rev. Lett. **72**, 1910 (1994).
[28]H. H. Wen, Z. X. Zhao, Y. G. Xiao, B. Yin, and J. W. Li, Physica C **251**, 371 (1995).